IMA Journal of Applied Mathematics (2015) Page 1 of 11
doi: 10.1093/imamat/dri017

Averaged dynamics of a coupled-inductor boost converter under sliding mode control using a piecewise linear complementarity model

NILIANA CARRERO*, CARLES BATLLE* AND ENRIC FOSSAS*
* *Institut d'Organització i Control de Sistemes Industrials [IOC]*
Universitat Politècnica de Catalunya [UPC],
Avda. Diagonal 647, 08028, Barcelona, Spain.

An averaged model of a coupled-inductor boost converter using the piecewise complementarity model of the converter under sliding motions is obtained. The model takes into account the idealized voltage-current characteristic of passive switches (diodes) present in the converter. Because of its lower complexity, the averaged model is more suitable for control design purposes as compared with the linear complementarity systems (LCS) model of the converter. The dynamic performance of the LCS model and the averaged models of the converter are validated through computer simulations using Matlab.

Keywords: linear complementarity system, sliding mode control, average dynamic, power converter

1. Introduction

Linear complementarity systems (LCS) (see Camlibel *et al.* (2003)) constitute an attractive alternative tool for modelling switching power converters (see Vasca *et al.* (2009)). Some of the main advantages are: 1) it does not require prior knowledge of all topological transitions that appear in the converter, 2) a single model is enough to capture the dynamics of the converter in both continuous conduction mode (CCM) and discontinuous conduction mode (DCM), and 3) it is a useful tool for converters with a large number of switching components. Motivated by these properties, the dynamics of a coupled-inductor boost converter using the LCS framework was obtained in Carrero *et al.* (2012). However, one of the major challenges in LCS modelling for power converters is robust and efficient control laws design. Sessa *et al.* (2014) present a general framework for describing power converters in closed-loop in the LCS formalism, yielding the complete closed loop dynamics in a compact form. The diodes and ideal switches are describe in LCS form. The control strategies considered are pulse width modulated (PWM) techniques and PI controllers. Those techniques were applied to the two basic dc-dc converters topologies (buck and boost) and to a Z-source converter. In Carrero *et al.* (2013) a cascade sliding mode-PID controller was designed for a piecewise complementarity model of a coupled-inductor boost converter. In spite of the fact that so far the mathematical formulation for using LCS models with sliding mode control has not been developed yet, both the simulation and experimental results (see Carrero *et al.* (2014)) showed an excellent performance and stable tracking with the proposed control law. Sliding mode control (SMC) is a variable structure control (VSC) technique widely used in control of power electronics due to the natural switching behaviour of the converters. In addition, it is well-known for its robustness against disturbances and parameter uncertainties. The latter property makes this technique a good candidate for robust control. In the classical theory of SMC (see Utkin *et al.* (2009) and Sira *et al.* (2006)) the derivation of a sliding mode control requires three steps. First, to define a discontinuous control law that locally forces the state trajectories to reach the sliding surface, yielding what is known as the reaching condition in the literature. Second, to design the control action necessary to maintain the sliding motion, or equivalent control. Third, to obtain the associated ideal sliding dynamics, or average

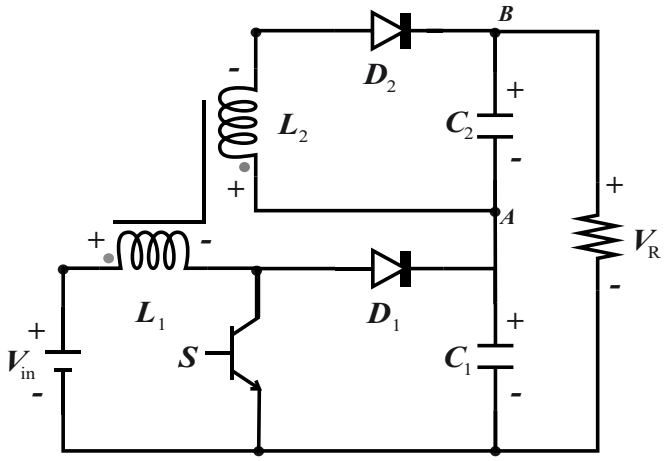

FIG. 1. Coupled-Inductor boost converter

dynamics. In this context, this paper focuses on obtaining an approximate average dynamics of the coupled-inductor boost converter by using the LCS model of the converter under sliding motion. This average dynamics can then be used for control purposes. Although the results presented in this paper do not constitute a formalization of the general theory for LCS under SMC, we think that they are a contribution to the design of robust control for LCS, which remains an open interesting problem.

The organization of the rest of the paper is as follows. Section 2 addresses the dynamic model of a coupled-inductor boost converter using the LCS framework. In Section 3 the control law proposed in Carrero *et al.* (2012) is presented, and an average dynamics based on the LCS model of the converter when sliding motions take place is obtained. Our approach is evaluated through computer simulation in Section 4, and the paper ends with some concluding remarks.

2. Modeling

2.1 *Linear complementarity model*

Let us consider the circuit of Figure 1, where the two inductors are coupled through a mutual inductance M. The state vector is defined as $\dot{x} = [i_{L_1}, i_{L_2}, v_{c_1}, v_{c_2}]^T$ which denote the currents through the inductors L_1 and L_2 and the voltages across the capacitors C_1 and C_2 respectively. In addition, it is desirable that $x_4 > 0$; if such condition is not satisfied then the converter under study does not offer any advantages over a conventional boost topology. Statements of the form $0 \leqslant a \perp b \leqslant b$, known as "complementarity conditions" (CC) (see Camlibel *et al.* (2003), Batlle *et al.* (2005)), mean that both a and b are non-negative and that if one of them is not zero, then the other one is zero. If a and b are vectors, then these conditions hold component-wise.

The LCS (see Vasca *et al.* (2009)) model of this circuit is given by Carrero *et al.* (2013)

- S=ON ($v_s = 0$)

$$\dot{x} = A_1 x + B_1 \omega + E_1 V_{in} \tag{2.1a}$$
$$z = C_1 x + D_1 \omega + F_1 V_{in} \tag{2.1b}$$
$$0 \leqslant z_1 \perp \omega_1 \geqslant 0 \tag{2.1c}$$
$$0 \leqslant z_2 \perp \omega_2 \geqslant 0 \tag{2.1d}$$

and the pairs of complementarity variables are given by

$$\omega_1 = i_{D1} \rightarrow z_1 = -v_{D1} = x_3 \tag{2.2a}$$
$$\omega_2 = -v_{D2} \rightarrow z_2 = i_{D2} = x_2 \tag{2.2b}$$

with

$$\begin{aligned} A_1 &= \begin{pmatrix} 0 & 0 & 0 & a_2 \\ 0 & 0 & 0 & -a_3 \\ 0 & 0 & -\frac{1}{C_1 R} & -\frac{1}{C_1 R} \\ 0 & \frac{1}{C_1} & -\frac{1}{C_2 R} & -\frac{1}{C_2 R} \end{pmatrix}, \; B_1 = \begin{pmatrix} 0 & -a_2 \\ 0 & a_3 \\ \frac{1}{C_1} & 0 \\ 0 & 0 \end{pmatrix}, \\ E_1 &= \begin{pmatrix} a_1 \\ -a_2 \\ 0 \\ 0 \end{pmatrix}, \; C_1 = \begin{pmatrix} 0 & 0 & 1 & 0 \\ 0 & 0 & 0 & 1 \end{pmatrix}, \\ D_1 &= \begin{pmatrix} 0 & 0 \\ 0 & 0 \end{pmatrix}, \; F_1 = \begin{pmatrix} 0 \\ 0 \end{pmatrix}, \end{aligned} \tag{2.3}$$

and

$$a_1 = \frac{L_2}{(L_1 L_2 - M^2)}, \; a_2 = \frac{M}{(L_1 L_2 - M^2)}, \; a_3 = \frac{L_1}{(L_1 L_2 - M^2)} \tag{2.4}$$

- S=OFF ($i_s = 0$)

$$\dot{x} = A_2 x + B_2 \omega + E_2 V_{in} \tag{2.5a}$$
$$z = C_2 x + D_2 \omega + F_2 V_{in} \tag{2.5b}$$
$$0 \leqslant z_1 \perp \omega_1 \geqslant 0 \tag{2.5c}$$
$$0 \leqslant z_2 \perp \omega_2 \geqslant 0 \tag{2.5d}$$

and the complementarity variables are given by the two pairs

$$\omega_1 = -v_{D1} \rightarrow z_1 = i_{D1} = x_1, \tag{2.6a}$$
$$\omega_2 = -v_{D2} \rightarrow z_2 = i_{D2} = x_2, \tag{2.6b}$$

with

$$\begin{aligned} A_2 &= \begin{pmatrix} 0 & 0 & -a_1 & a_2 \\ 0 & 0 & a_2 & -a_3 \\ \frac{1}{C_1} & 0 & -\frac{1}{C_1 R} & -\frac{1}{C_1 R} \\ 0 & \frac{1}{C_2} & -\frac{1}{C_2 R} & -\frac{1}{C_2 R} \end{pmatrix}, \; B_2 = \begin{pmatrix} a_1 & -a_2 \\ -a_2 & a_3 \\ 0 & 0 \\ 0 & 0 \end{pmatrix}, \\ E_2 &= E_1, \;\; C_2 = \begin{pmatrix} 1 & 0 & 0 & 0 \\ 0 & 1 & 0 & 0 \end{pmatrix} \end{aligned} \tag{2.7}$$

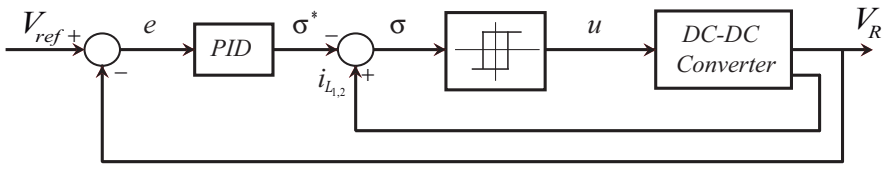

FIG. 2. Feedback control scheme for the coupled-inductor boost converter

Notice that the second pair of complementarity variables in (2.2b) and (2.6b) remain the same for both positions of the switch, while the first pair in (2.2a) is the opposite of the pair in (2.6a). Thus in compact form, the dynamics of the converter can then be rewritten as

$$\begin{aligned} \dot{x} &= A_1 x + B_1 \omega + E_1 V_{in} + (\mathrm{A}x + \mathrm{B}\omega + \mathrm{E}V_{in})\, u \\ z &= C_1 x + D_1 \omega + F_1 V_{in} + (\mathrm{C}x + \mathrm{D}\omega + \mathrm{F}\mathrm{V}_{\mathrm{in}})\, u \\ & 0 \leqslant \omega \perp z \geqslant 0 \\ u &= \begin{cases} 1 & \rightarrow \quad \mathrm{S = ON} \\ 0 & \rightarrow \quad \mathrm{S = OFF} \end{cases} \end{aligned} \tag{2.8}$$

where $\mathrm{A} = A_2 - A_1$, $\mathrm{B} = B_2 - B_1$, $\mathrm{C} = C_2 - C_1$, $\mathrm{D} = D_2 - D_1$, $\mathrm{E} = E_2 - E_1$ and $\mathrm{F} = F_2 - F_1$.

3. Control

Due to the complexity of control design for the LCS model of the converter presented in the above section, we propose, as a trade off, to obtain an average dynamics of the converter by using the LCS model. The main control objective is to maintain the output voltage close to a desired reference value. At the same time, this control must be carried out in the presence of load variations, voltage disturbance and limitations on the manipulated variable (duty cycle). In Carrero *et al.* (2013) a cascade control law was presented to achieve these goals. The general architecture of the feedback control law is shown in Figure 2. The inner loop was based on a non-linear control strategy similar to sliding mode control, with the goal of controlling the inductors currents. The switching surface $\sigma(x) = 0$ is given by

$$\sigma(x) = \alpha_1 x_1 + \alpha_2 x_2 - \sigma^* \tag{3.1}$$

where $\alpha_1 = L_1 \alpha_0$, $\alpha_2 = M\alpha_0$, $\alpha_0 = \sqrt{(L_1 L_2 - M^2)/C_1}\,\Big/ V_{in}$ and σ^* is the signal reference provided by the PID controller designed for the outer loop in order to control the output voltage. The rule for the switch is given by

$$u = \begin{cases} 1 & if \quad \sigma(x) < 0 \\ 0 & if \quad \sigma(x) > 0 \end{cases} \tag{3.2}$$

where u represents the switch position. The attractiveness of the sliding surface was proven in Carrero *et al.* (2013). Our goal is to obtain a simplified, averaged model for the inner closed loop in Figure 2, assuming that sliding motion has been reached. According to Utkin's mathematical analysis, the average or ideal sliding dynamics is defined by $\sigma = 0$ and $\left\langle \nabla\sigma, f(t,x,\omega,u_{eq}) \right\rangle = 0$, where f is the vector field

given in (2.8) but with the control law u been replaced by the control under sliding mode u_{eq}. $\nabla\sigma$ denotes the gradient of $\sigma(x)$ and $\langle,\rangle$ is the standard scalar product of vectors. One gets $u_{eq} = V_{in}/(x_3 - \omega_1)$, which depends on the complementarity variable ω_1. Notice that this ω_1 has physical dimensions of voltage and thus is the one defined by (2.6a). It is easy to see from the equivalent control that a necessary condition for the existence of a sliding mode on $\sigma = 0$ is $\omega_1 \neq x_3$. This condition is called transversal condition (see Utkin *et al.* (2009)). Replacing u_{eq} in (2.8) yields a nonlinear complementarity system and, in fact, an additional nonlinearity is introduced by means of an hysteresis used to implement the switching action. Hence, the ideal sliding dynamics is not an LCS, and it is in this context that the authors propose to analyze the piece-wise linear complementarity system when σ has a periodic behavior in order to obtain the dynamics that takes place when the sliding regime is reached. This will be addressed in the following section and results in a good approximation.

3.1 *Average model*

According to the control objectives, one must regulate the third and fourth components of the complementarity model (2.1) and (2.5),

- S=ON ($v_s = 0$)

$$\begin{cases} \dot{x}_3 = \dfrac{1}{C_1}\omega_1 - \dfrac{x_3 + x_4}{RC_1} \\ \dot{x}_4 = \dfrac{1}{C_2}x_2 - \dfrac{x_3 + x_4}{RC_2} \quad if \quad 0 < t \leqslant dT \\ 0 \leqslant z \perp \omega \geqslant 0 \end{cases} \tag{3.3}$$

- S=OFF ($i_s = 0$)

$$\begin{cases} \dot{x}_3 = \dfrac{1}{C_1}x_1 - \dfrac{x_3 + x_4}{RC_1} \\ \dot{x}_4 = \dfrac{1}{C_2}x_2 - \dfrac{x_3 + x_4}{RC_2} \quad if \quad dT < t \leqslant T \\ 0 \leqslant \hat{z} \perp \hat{\omega} \geqslant 0 \end{cases} \tag{3.4}$$

where the duty cycle d is the fraction of time in which the switch S is in the ON state. This variable may be interpreted as the average of the discontinuous control law in (3.2). The dynamics of x_4 is independent of the switch position, but that of x_3 depends on the complementarity variable ω_1 and the inductor current x_1. From the complementarity restriction in (2.2a) it follows that $\omega_1 = 0$, since z_1 is an output voltage that must be different from zero. This means that, when computing the average dynamics of x_3, it suffices to average x_1 in the OFF state. Notice that the inductor current x_1 is equal to the current through the diode D_1 during the fraction of time that the switch is in the OFF state, while the inductor current x_2 is equal to the current through the diode D_2 during the entire switching period.

Using the averaging theory for hybrid systems (see Teel *et al.* (2010) and Pedicini *et al.* (2011)), the average model of the output voltage can be written in the following form

$$\dot{\bar{x}} = f_2 + (f_1 - f_2)d, \quad \bar{x} = (\bar{x}_3\ \bar{x}_4)^T, \tag{3.5}$$

where f_1 and f_2 are averaged vector fields for the ON and OFF states respectively, and where x_1 and x_2 are to be replaced by averaged values $x_1 \cong \bar{x}_1(x_3, x_4)$ and $x_2 \cong \bar{x}_2(x_3, x_4)$, given in terms of the variables x_3, x_4.

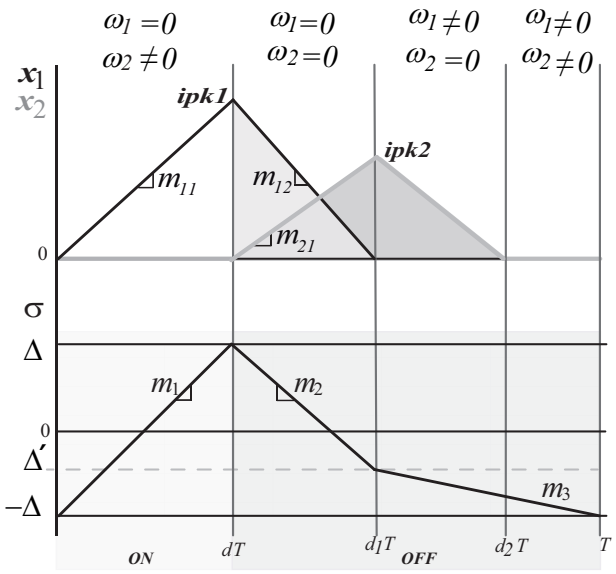

FIG. 3. Waveforms of the inductors currents and sliding surface in one switching period. See the appendix for the values of the parameters.

We focus on the dynamical behaviour of the inductor currents when sliding motion occurs, in order to obtain its average. This behaviour is illustrated in Figure 3. It is worth noting that when $\sigma(x)$ reaches a periodic regime so do the inductor currents. Additionally it can be seen from this figure that the inductor currents are zero for a portion of the switching cycle, and hence the converter is working in DCM (see Erickson *et al.* (2001)). The reader is referred to Carrero *et al.* (2012) to explore other behaviours of the inductor currents trajectories in steady state that appear in this converter. The average value of the primary inductor current over one switching period is given by the area under its curve, which is equivalent to the area of the triangle with height i_{pk_1} and base length d_1T (see Figure 3). In a similar way, the average value of the secondary inductor current is obtained from the area of the triangle with height i_{pk_2} and base length $(d_2-d)T$. One has

$$\bar{x}_1 = \frac{1}{T}\int_0^T x_1(t)dt = \frac{i_{pk_1}d_1}{2} = \bar{x}_1(x_3,x_4), \tag{3.6}$$

$$\bar{x}_2 = \frac{1}{T}\int_0^T x_2(t)dt = \frac{i_{pk_2}(d_2-d)}{2} = \bar{x}_2(x_3,x_4). \tag{3.7}$$

Next, the average currents through the diodes D_1 and D_2 can be expressed as the areas of the shaded triangles in Figure 3,

$$\bar{i}_{D_1} = \frac{1}{T}\int_{dT}^{T} x_1(t)dt = \frac{i_{pk_1}(d_1-d)}{2} = \bar{i}_{D_1}(x_3,x_4), \tag{3.8}$$

$$\bar{i}_{D_2} = \frac{1}{T}\int_{0}^{T} x_2(t)dt = \frac{i_{pk_2}(d_2-d)}{2} = \bar{i}_{D_2}(x_3,x_4). \tag{3.9}$$

Summing up, the average dynamics that describes the output voltage of the converter when the sliding surface is reached can be written as

$$\begin{aligned} \dot{\bar{x}}_3 &= \frac{1}{C_1}\bar{i}_{D_1}(\bar{x}_3,\bar{x}_4) - \frac{\bar{x}_3+\bar{x}_4}{RC_1} \\ \dot{\bar{x}}_4 &= \frac{1}{C_2}\bar{x}_2(\bar{x}_3,\bar{x}_4) - \frac{\bar{x}_3+\bar{x}_4}{RC_2} \end{aligned} \tag{3.10}$$

The expressions of i_{pk_1}, i_{pk_2}, d, d_1, d_2 and T in terms of $x_3 \approx \bar{x}_3$ and $x_4 \approx \bar{x}_4$ and of the parameters of the circuit and of the sliding surface are derived in Appendix A.

Since the voltages across C_1 and C_2 are assumed to be constant, we can write $x_3 \approx \bar{x}_3$ and $x_4 \approx \bar{x}_4$ (see Erickson *et al.* (2001)). In this way, we obtain a simplified model for the inner loop in Figure 2. Furthermore the equilibrium point of the second order model, which is locally stable, coincide with the desired voltage values. Therefore after applying the Jacobian linearization method to this second order model, the resulting model can be used to tune the PID control of the outer loop, resulting in a simpler control design procedure.

4. Simulation results

This section provides the simulation results of the linear complementarity model defined in (2.1) and (2.5) under sliding mode control and the results correspond to the average model defined in (3.10). Both models were implemented using Matlab. For the LCS model the back-Euler method plus a specific solution of the linear complementarity problem (LCP) was used, while Matlab's standard solver was used for the average model. The nominal values of the converter parameters are $V_{in} = 12V$, $L_1 = 75e-6H$, $L_2 = 525e-6H$, $M = 168e-6H$, $C_1 = 22e-6F$, $C_2 = 22e-6F$, $R = 100\Omega$, the hysteresis thresholds are $\Delta = \pm 29e-8$ and we are assuming that the reference of the current loop is a constant value $\sigma^* = 2.9e-7$. The initial conditions for both models are $x = [0,0,0,0]^T$ and $\bar{x} = [15,0]^T$, respectively. Figure 4 shows the computer simulation results. From the sliding surface trajectory (see Figure 4(c)), it is evident that the existence and reaching conditions for having sliding modes are satisfied, since $(\sigma(x))(\dot{\sigma}(x)) < 0$. On the other hand, as can be seen from the average trajectory in Figure 4(d) (red curve), it is quite close to the result produced by the LCS model (blue curve) during the steady state. The error of the average dynamics with respect to the LCS model in the steady state is less than 3%, and it is somehow higher during the transient. This is to be expected, due to the many assumptions and approximations carried out in order to obtain the average of the output voltage. Notice that, in particular, it has been assumed that σ has a periodic behaviour, and this is not necessarily true during the transient. In our opinion, the advantages of the simplified control design procedure of the proposed method overcome the loss of accuracy in the resulting model.

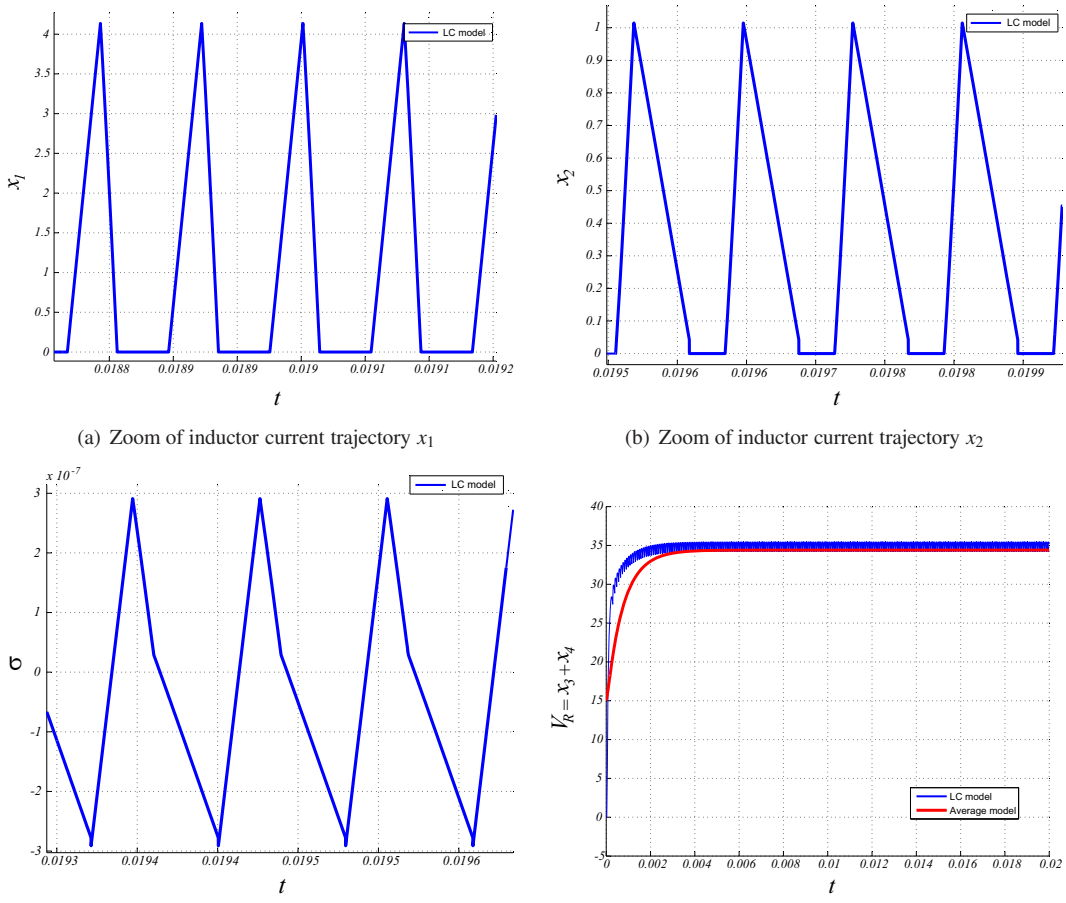

(a) Zoom of inductor current trajectory x_1

(b) Zoom of inductor current trajectory x_2

(c) Zoom of sliding surface trajectory $\sigma(x)$

(d) Output voltage trajectory $v_R = x_3 + x_4$

FIG. 4. Simulation results. Figures 4(a) and 4(b) display the waveforms of the inductor currents for the LCS model, while Figure 4(c) displays the sliding surface. Figure 4(d) shows the output voltage for the LCS (blue trace) and averaged (red trace) models.

5. Concluding remarks

In this paper we have addressed a very interesting challenge of deriving the averaged dynamics of a coupled-inductor boost converter through a piecewise complementarity model of the converter when sliding motion occurs. This latter model takes into account the hybrid dynamics of switching components. Even though the general mathematical formulation for LCS under sliding motion has not been developed, the approach used shows, by means of computer simulations, that the averaged dynamics yields a good approximation of the more complex LCS model of the converter when sliding motions take place. The averaged model is a second order system that simplifies the control design for the coupled-inductor boost converter. Even though we have not presented a general analysis for LCS under SMC, we think nevertheless that these ideas constitute a very promising starting point for the analysis of the ideal sliding trajectory in LCS. Future research work will deal with a more general analysis of the averaged dynamics for LCS and the stability analysis under sliding mode.

Acknowledgements

The work of CB and EF was partially supported by Generalitat de Catalunya through project 2014 SGR 267, and CB was also supported by CICyT project DPI2015-69286-C3-2-R.

References

CARRERO, N., BATLLE, C. & FOSSAS, E. (2013). Cascade sliding mode-PID controller for a coupled-inductor boost converter, *Decision and Control (CDC), 2013 IEEE 52nd Annual Conference on*, 3653–3658.

CAMLIBEL, M.K., HEEMELS, W.P.M.H., VAN DER SCHAFT, A.J & SCHUMACHER, J.M. (2003). Switched Networks and Complementarity, *Circuits and Systems I, IEEE Transactions on*, **50**, 1036–1046.

BATLLE, C., FOSSAS, E., MERILLAS, I. & MIRALLES, A. (2005). Generalized Discontinuous Conduction Modes in the Complementarity Formalism, *Circuits and Systems II: Express Briefs, IEEE Transactions on*, **52**, 447–451.

PEDICINI, C., VASCA, F., IANNELLI, L. & JONSSON, U. (2011). An overview on averaging for pulse-modulated switched systems, *Decision and Control and European Control Conference (CDC-ECC), 2011 50th IEEE Conference on*, 1860 –1865.

TEEL, A.R, VASCA & NESIC, D (2010). PWM hybrid control systems: averaging tools for analysis and design, *Control Applications (CCA), 2010 IEEE International Conference on*, 1128–1133.

CARRERO, N., BATLLE, C. & FOSSAS, E. (2012). Modeling a Coupled-Inductor boost Converter in the Complementarity Framework, *Computer Modeling and Simulation (EMS), 2012 Sixth UKSim/AMSS European Symposium on*, 471–476.

ERICKSON, R. W. & MAKSIMOVIC, D. (2001). Fundamentals of Power Electronics, 2nd ed. 2001, XXI, 883.

VASCA, F., IANNELLI L., CAMLIBEL M. K. & FRASCA, R. (2009). A New Perspective for Modeling Power Electronics Converters: Complementarity Framework, Power Electronics, IEEE Transactions on, 456–468.

COTTLE, R., PAN J.S., & STONE, R. (1992). The Linear Complementarity Problem, Academic Press, New York, 762.

SESSA, V, IANNELLI L. & VASCA, F (2014). A Complementarity Model for Closed-Loop Power Converters, Power Electronics, IEEE Transactions on, **29** 6821–6835.

CARRERO, N., BATLLE, C. & FOSSAS, E. (2014). Experimental evaluation of a cascade sliding mode-PI controller for a coupled-inductor boost converter, *Variable Structure Systems (VSS), 2014 13th International Workshop on*, 1–6.

UTKIN, V., GULDNER, J. & SHI, J. (2009). Sliding Mode Control in Electro-mechanical Systems (Automation and Control Engineering, *CRC Press Inc; Edicin: 2nd Revised edition*.

SIRA-RAMIREZ, H. J. & ILVA-ORTIGOZA, R. (2006). Control Design Techniques in Power Electronics Devices,

Springer London Ltd.

A. Average currents

In order to analyse the inductor currents trajectories together with the sliding surface in Figure 3, the switching period is divided into subintervals of time.

- $[0 - dT]$
  During the interval of time in which the switch is in On position, one gets

$$\dot{\sigma} = m_1 = \sqrt{\frac{L_1 L_2 - M^2}{C_1}} \tag{A.1}$$

  From the sliding surface trajectory one gets that the value of the duty cycle is given by

$$d = \frac{2\Delta}{T m_1} \tag{A.2}$$

  On the other hand, because the inductor current x_2 is constant, its derivative will be zero during this subinterval. Hence, the inductor current change $\dot{x}_1$ is obtained by substituting $\dot{x}_2 = 0$ in $\dot{s} = \alpha_1 \dot{x}_1 + \alpha_2 \dot{x}_2$. Equating this to (A.1) one gets

$$\dot{x}_1 = m_{11} = \frac{V_{in}}{L_1} \tag{A.3}$$

  Thus the maximum value of the inductor current x_1 at the end of the interval of time is given by

$$i_{pk_1} = m_{11} dT \tag{A.4}$$

- $[dT - d_1 T]$
  The change of the inductors currents are obtained from the first and the second components of the vector field in (2.5), yielding

$$\dot{x}_1 = m_{12} = a_1 x_3 + a_2 x_4 + a_1 V_{in} \tag{A.5}$$
$$\dot{x}_2 = m_{21} = a_2 x_3 - a_3 x_4 - a_2 V_{in} \tag{A.6}$$

  The maximum values of the inductors currents x_1 and x_2 are given by

$$i_{pk_1} = -m_{12}(d_1 - d)T \tag{A.7}$$
$$i_{pk_2} = -m_{21}(d_1 - d)T \tag{A.8}$$

- $[d_1 T - d_2 T]$
  The derivative of the sliding surface is given by

$$\dot{\sigma} = m_3 = \sqrt{\frac{L_1 L_2 - M^2}{C_1 V_{in}^2}}(V_{in} + \omega_1 - x_3) \tag{A.9}$$

Note that the primary inductor current is constant during this subinterval. Replacing $\dot{x}_1 = 0$ in $\dot{\sigma} = \alpha_1 \dot{x}_1 + \alpha_2 \dot{x}_2 = m_3$ and $\dot{x}_2$ by the second component of the vector field in (2.5) and solving this for ω_1 one gets

$$\hat{\omega}_1 = -\frac{V_{in}L_2 + Mx_4 - L_2 x_3}{L_2} \tag{A.10}$$

In addition, the value that takes the sliding surface at the beginning of this interval of time is obtained by replacing $x_1 = 0$ and $x_2 = i_{pk_2}$ in (3.1). Thus one gets

$$\Delta^{'} = \alpha_2 i_{pk_2} - \sigma^* \tag{A.11}$$

- $[d_2 T - T]$
  The switching period is given by

$$T = d_2 - \frac{\Delta + \Delta^{'}}{m_3} \tag{A.12}$$

Solving for i_{pk_1}, i_{pk_2}, d_1, d_2 and T from the previous equations one obtains

$$\begin{aligned}
i_{pk_1} &= \frac{2V_{in}\Delta}{L_1\sqrt{\frac{L_1L_2-M^2}{C_1}}}, \\
i_{pk_2} &= \frac{2V_{in}\Delta\,(MV_{in} + L_1x_4 - Mx_3)}{L_1\sqrt{\frac{L_1L_2-M^2}{C_1}}(L_2V_{in} + Mx_4 - L_2x_3)}, \\
d &= \frac{2\Delta ML_1x_4}{(L_1L_2(\Delta-\sigma^*) + 2\Delta M^2)V_{in} + 2\Delta ML_1x_4}, \\
d_1 &= \frac{2\Delta Mx_4(V_{in}M^2 + L_1Mx_4 - L_1L_2x_3)}{(L_2V_{in} + Mx_4 - L_2x_3)((L_1L_2(\Delta-\sigma^*) + 2\Delta M^2)V_{in} + 2\Delta ML_1x_4)}, \\
d_2 &= \frac{2\Delta M(V_{in}M + L_1x_4)}{(L_1L_2(\Delta-\sigma^*) + 2\Delta M^2)V_{in} + 2\Delta ML_1x_4}, \\
T &= \frac{\sqrt{C_1(L_1L_2-M^2)}((L_1L_2(\Delta-\sigma^*) + 2\Delta M^2)V_{in} + 2\Delta ML_1x_4)}{(L_1L_2-M^2)ML_1x_4}.
\end{aligned} \tag{A.13}$$